# Accepted Manuscript

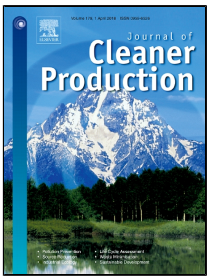


Development of natural fiber-reinforced composite with comparable mechanical properties and reduced energy consumption and environmental impacts for replacing automotive glass-fiber sheet molding compound

Yingji Wu, Changlei Xia, Liping Cai, Andres C. Garcia, Sheldon Q. Shi

| | |
|---|---|
| PII: | S0959-6526(18)30589-4 |
| DOI: | 10.1016/j.jclepro.2018.02.257 |
| Reference: | JCLP 12204 |
| To appear in: | *Journal of Cleaner Production* |
| Received Date: | 03 August 2017 |
| Revised Date: | 19 February 2018 |
| Accepted Date: | 23 February 2018 |

Please cite this article as: Yingji Wu, Changlei Xia, Liping Cai, Andres C. Garcia, Sheldon Q. Shi, Development of natural fiber-reinforced composite with comparable mechanical properties and reduced energy consumption and environmental impacts for replacing automotive glass-fiber sheet molding compound, *Journal of Cleaner Production* (2018), doi: 10.1016/j.jclepro.2018.02.257

# Development of natural fiber-reinforced composite with comparable mechanical properties and reduced energy consumption and environmental impacts for replacing automotive glass-fiber sheet molding compound

*Yingji Wu, Changlei Xia*, Liping Cai, Andres C. Garcia, Sheldon Q. Shi**

## Graphical Abstract

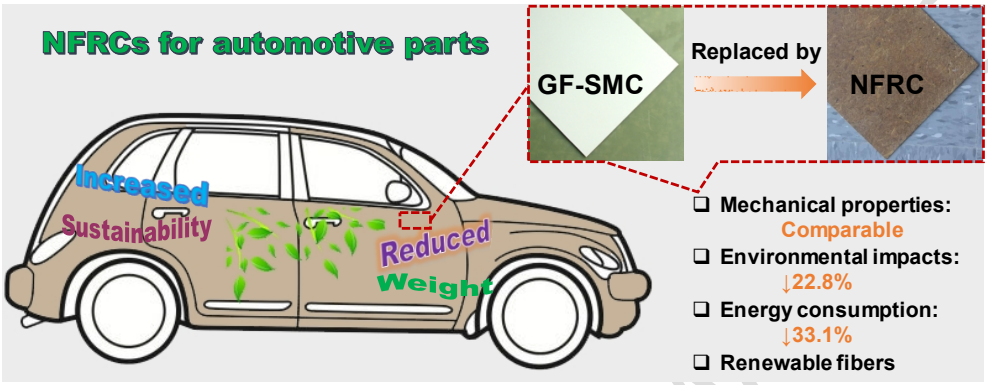

**Word Counts: 7030**

# Development of natural fiber-reinforced composite with comparable mechanical properties and reduced energy consumption and environmental impacts for replacing automotive glass-fiber sheet molding compound

*Yingji Wu*[a], *Changlei Xia*[*,a,b], *Liping Cai*[a,b], *Andres C. Garcia*[c], *Sheldon Q. Shi*[*,a]

[a] Department of Mechanical and Energy Engineering, University of North Texas, Denton, TX 76203, USA

[b] College of Materials Science and Engineering, Nanjing Forestry University, Nanjing, Jiangsu 210037, China

[c] Department of Mechanical Engineering, The University of Texas at Tyler, Tyler, TX 75799, USA

*Corresponding authors.

C. Xia: E-mail: cx0014@unt.edu

S. Q. Shi: Tel.: +1 9403695930; Fax: +1 9403698675; E-mail: Sheldon.Shi@unt.edu

**Abstract**

To replace glass-fiber sheet molding compound (GF-SMC) using natural fiber-reinforced composites (NFRCs) in the automotive industry, this work intended to enhance mechanical properties and water resistance of NFRCs by impregnating magnesium hydroxide (MH) to kenaf fibers and fabricating composites using the vacuum bag resin transfer molding (VBRTM) technology. The modulus of rupture and tensile strength of modified composites were significantly increased by 73.9% and 54.6% compared with that of the regular NFRCs, respectively. Based on the scanning electron microscope observation, it was found that the MH impregnation significantly enhanced the compatibility of kenaf fibers and polymer matrix, benefiting to the mechanical-property improvements of the composites. Compared to the regular NFRC, the 24-h water absorption and thickness swelling of MH impregnated NFRC (MH-NFRC) were significantly reduced by 83.9% and 84.2%, respectively. When the composite density was factored in the comparison of MH-NFRC and GF-SMC, the specific modulus of rupture and tensile strength of MH-NFRC were 116.4% and 109.0% of the GF-SMC, respectively. Apart from the mechanical properties, the advantages of replacing GF-SMC by MH-NFRC were reflected in the reductions of energy consumption and environmental impacts. It was calculated that the energy consumption of fabricating MH-NFRC was decreased by 33.1% compared with GF-SMC. The comparisons of environmental impacts of MH-NFRC and GF-SMC were performed by life-cycle assessment (LCA) using the SimaPro software. The results demonstrated that the environmental burdens of the composites were reduced by 22.8%, when kenaf fibers were used. All major indices of environmental impacts of MH-NFRC, including the total Global warming, Acidification, Human Health (HH) cancer, HH noncancer, HH criteria air pollutants, Eutrophication, Ecotoxicity, Smog, Natural resource depletion, Habitat alteration, Water intake and Ozone depletion, were reduced by 13.66 – 51.91%, respectively. It was concluded that the newly developed NFRC had great potential for replacing the GF-SMC in automobile applications, with reduced energy consumption and environmental impacts.

***Keywords:*** Natural fibers; Magnesium hydroxide; Vacuum bag resin transfer molding (VBRTM); Glass-fiber sheet molding compound (GF-SMC); Automotive application; Life-cycle assessment (LCA)

**Nomenclature list**

| | |
|---|---|
| ANOVA | Analysis of variance |
| $Ash_{Mg(OH)2/fiber}$ | Ash content of magnesium hydroxide impregnated fibers |
| $Ash_{fiber}$ | Ash content of control kenaf fiber |
| $CaCO_3$ | Calcium carbonate |
| $C_{Mg(OH)2}$ | Magnesium hydroxide content of magnesium hydroxide impregnated fibers |
| EMI | Electromagnetic interference |
| GF | Glass fiber |
| GF-SMC | Glass-fiber sheet molding compound |
| HH | Human health |
| LCA | Life-cycle assessment |
| $MgCl_2$ | Magnesium chloride |
| MgO | Magnesium oxide |
| $Mg(OH)_2$ | Magnesium hydroxide |
| MH | Magnesium hydroxide |
| MH-NF | Magnesium hydroxide impregnated natural fiber |
| MH-NFRC | Magnesium hydroxide impregnated natural fiber-reinforced composite |
| $M_{MgO}$ | Molecular weight of magnesium oxide |
| $M_{Mg(OH)2}$ | Molecular weight of magnesium hydroxide |
| NaOH | Sodium hydroxide |
| NF | Natural fiber |
| NFRC | Natural fiber-reinforced composite |
| PP | Polypropylene |
| SEM | Scanning electron microscope |
| t-BP | tert-Butyl peroxybenzoate |
| TGA | Thermal gravity analysis |
| TS | Thickness swellings |
| UPR | Unsaturated polyester resin |
| VBRTM | Vacuum bag resin transfer molding |
| WA | Water absorptions |

## 1. Introduction

Due to the increasing concern with the environment and sustainability, natural fibers (NFs) are increasingly utilized owing to their excellently sustainable, biodegradable, eco-friendly and economic properties (Vaisanen et al., 2017). Natural fiber-based composites (NFRCs) have shown outstanding mechanical properties comparable to those of glass-fiber sheet molding compound (GF-SMC) (Koronis et al., 2013). Apart from the application of composites, NFs have been used for NF reinforced tubes (Yan and Chouw, 2014), carbon materials (Xia and Shi, 2016), NF filled cement (Claramunt et al., 2016), thermal-conductivity enhancing materials (Xia et al., 2016c), electromagnetic interference (EMI) shielding materials (Xia et al., 2017), EMI absorption materials (Xia et al., 2016b), etc. Recently, a few primary studies have been performed to use NFRCs in automotive industries initially by the Europeans (Dahlke et al., 1998), and then followed by Canadians (Pervaiz and Sain, 2003), Americans (Holbery and Houston, 2006), Malaysia (AL-Oqla and Sapuan, 2014), etc. In a feature article, Marsh pointed out the next step for automobile materials using NFs and bio-based resin (Marsh, 2003). These studies were mainly focusing on the theoretical studies, e.g. environmental benefit, energy conserving, sustainability and prospect, but few investigations on the NFRCs' mechanical properties to be used in automobiles (Vaisanen et al., 2017).

As one of renewable NF resources, the kenaf (*Hibiscus cannabinus, L. Malvaceae*) fiber utilization is placed high on the priority list because of the large quantities of kenaf existing and available for producing value-added products (Zamri et al., 2016). Driven by its eco-friendly properties and excellent characteristics of economy, kenaf fiber composites have been rapidly developed recently (Akil et al., 2011). It has been found that the bonding strength of the interface between fibers and polymer has been a major concern because of pendant polar groups (e.g. hydroxyl) in NFs (Bledzki et al., 2005), leading to high water uptake of NFs and resulting in poor mechanical performance of NFRCs (Pickering et al., 2016). Chemical/physical modifications of the fibers have been investigated to reduce the hydrophilic behavior of fibers and the moisture absorption of their composites (Chandrasekar et al., 2017). As a non-toxic and economical resource, calcium carbonate (Xia et al., 2015b) and nano-calcium carbonate (Wang et al., 2017) were wildly used to modify the NFs for improving properties of kenaf fiber composites.

The vacuum bag resin transfer molding (VBRTM) is considered as an ideal technology for processing large structures (e.g. boat and automotive parts), and endowed the advantages, like lower tooling costs, and possible for room temperature processing (Sadeghian et al., 2006). The high-performance composite components for the wind energy and marine markets were fabricated using the VBRTM process. Most commonly, synthetic fibers, e.g. glass fibers (GFs) (Chen et al., 2017) and carbon fibers (Mendonca Sales et al., 2017), were used to make high-performance composites through the VBRTM process. Recently, the VBRTM process was used to produce NFRCs to improve the mechanical performance (Xia et al., 2015a). The reason could be that the porosity of the NFRC was dramatically reduced by means of VBRTM process.

Limited studies regarding the utilization of magnesium hydroxide (MH) for property modification of composites were found in the literature review. Zhu et al. (2011) successfully grew the MH films on AZ31 magnesium alloy substrates by means of the hydrothermal method. After being coated with MH films, the corrosion resistance of the alloy was significantly improved. The results indicated that of the MH film formation on the surfaces of AZ31 magnesium alloy could offer a potential stock for appropriate orthopedic surgery. Koh et al. (2011) effectively deposited the MH nanopetals on the surfaces of zeolite 4Å at 298 K by the addition of ammonium hydroxide to magnesium chloride

aqueous solution and concluded that it could be possible to control the size and composition of MH/zeolite 4Å nanocomposites.

Life-cycle assessment (LCA) can evaluate environmental impacts, including the emissions into the environment and the consumption of resources, as well as the land use (Rebitzer et al., 2004), which contributes to overall environmental impacts, such as climate change, stratospheric ozone depletion, tropospheric ozone, eutrophication, acidification, toxicological stress on human health and ecosystems, etc. Korol et al. (2016) compared the environmental assessment of a plastic pallet produced from selected bio-composites and composites based on the ReCiPe using the LCA method. Furthermore, the environmental assessment findings were used for quantification of the eco-efficiency and confirmed that the environmental impact categories were related to the eco-efficiency results. Boonterm et al. (2016) compared the environmental impacts of rice straw thermal insulation pads produced by different cellulose extraction processes using LCA. It was found that the thermal steam explosion process had lower environmental impacts than the chemical extraction treatment because of the lower eco-toxicity impact and a higher fiber yield. However, the thermal explosion process had the drawback of higher energy consumption. La Rosa et al. (2014) completed a comparative LCA between an eco-sandwich made of bio-based epoxy resin (SuperSap 100/1000) and NFs against a traditional sandwich made of epoxy/glass-fibers. LCA results illustrated that bio-based polymers presented more favorable environmental impacts and energy use compared to petroleum-based products. Ardente et al. (2008) investigated the life-cycle impacts of kenaf board by comparing to the performances of various replaceable products, as polyurethane, glass wool, flax rolls, stone wool, mineral wool and paper wool. It was found that the highest impacts were related to synthetic materials, while the better performances were due to mineral wools.

Alves et al. (2010) utilized natural jute fibers to replace glass fibers to produce a structural frontal bonnet of an off-road vehicle and presented several social, environmental and economic advantages through LCA method. Ashori (2008) fabricated wood–plastic composite, which was a sustainable green material without using toxic chemicals. AL-Oqla and Sapuan (2014) used the date palm fibers (DPF) to make fiber reinforced polymer composites for automotive industry. Their study provided the mechanical properties of individual fibers and compared to conventional polymers. To ensure the competitiveness of DPF in fabrication of composites the automotive industry, a comparison between DPF and other fibers was conducted and concluded that DPF was the best selected fiber among all other types. However, the previously described reports did not present the mechanical properties of the prepared natural fiber composites and the comparison with the automotive glass-fiber sheet molding compound (SMC).

The literature review does not discover any study regarding the NFRCs manufacturing by means of MH-impregnated kenaf fibers using the VBRTM process. This research is aimed to find the viability of the use of NFRCs in the fabrication of some automotive components. By using the MH-impregnated kenaf fibers and VBRTM, the water resistance and mechanical properties of NFRCs were significantly improved, which can be comparable with commercially available GF-SMC used as outer door, roof bow, and front roof panels. In this study, a novel process for high-performance NFRCs was successfully developed. The effect of MH content on the composite properties were examined. The comparison of energy consumption between NFRC and GF-SMC was estimated. In addition, the LCA comparison of NFRC and GF-SMC was completed based on the ISO 14040 standard of LCA framework, which was employed to present the environmental advantages of using NFRV to replace GF-SMC.

## 2. Materials and Methods

Provided by Kengro Corp. (USA), original kenaf (*Hibiscus cannabinus* L.) bast fibers were chopped into shorter fibers with a length of approximate 50.8 mm (2 inch). The 5% (w/v) Sodium hydroxide (NaOH) aqueous solution was prepared from NaOH beads (purity ≥97%, Acros Organics). The solutions of magnesium chloride ($MgCl_2$) were prepared using $MgCl_2 \cdot 6H_2O$ (99%, Sigma-Aldrich). The unsaturated polyester resin (UPR) was provided by Ashland Chemicals, USA, which contained 30% styrene. The tert-butyl peroxybenzoate (t-BP, purity = 98%) was purchased from Acros Organics, USA.

### *2.1. In-situ magnesium hydroxide impregnation*

Kenaf fibers (100 g, 9.11% moisture content) was fed into the Parr reactor (251 M) and mixed with 1.8 L NaOH (5%, w/v) aqueous solution (Xia et al., 2015a). The mixture was conducted to alkali retting process with a temperature of 160 °C, calculating the vapor pressure to be approximate 0.60 MPa. The retting system self-cooled to room temperature after mechanical stirring for one hour. To remove the excessive ionic solution from the mixture, gravity was used firstly and then hand-squeezed. The retted kenaf fibers were then washed by distilled water for several times until the water *p*H value close to 7. The yields of treated kenaf fibers were measured to be 36.6 ± 1.2%.

The *in-situ* loading of MH was conducted by mixing the fresh retted kenaf fibers and 1 L $MgCl_2$ aqueous solutions into the Parr reactor, with various concentrations (0.05/0.1/0.2/0.4 mol $L^{-1}$). After heating to 100 °C (the vapor pressure of approximately 0.10 MPa), the hermetical reactor maintained the temperature for 0.5 h. After self-cooling to approximate 35 °C, 0.8 L NaOH solutions with different concentrations (0.125, 0.25, 0.5, and 1 mol $L^{-1}$, respectively) were poured into the reactor and heated at 100 °C for another 0.5 h. The following reaction occurred in-situ to form MH particles in and on the kenaf fibers.

$$MgCl_2 + 2NaOH \rightarrow Mg(OH)_2\downarrow + 2NaCl \quad (1)$$

After self-cooling to approximately 25 °C, the modified kenaf fibers were filtered and then distilled-water washed to be neutralizing. The modified kenaf fibers were dried at 105 °C for 24 hours to form mat preforms, which had dimensions of approximate 100 × 165 × 10 mm (width × length × thickness) for the VBRTM process.

### *2.2. Magnesium hydroxide content determination*

In terms of the difference of ash contents of the retted fibers and magnesium hydroxide impregnated natural fibers (MH-NFs), the MH contents were calculated. The fibers were burned in an oven at 675 °C for 6 h, the ash contents were determined accordingly. The thermal gravity analysis (TGA) data showed that the MH was decomposed into magnesium oxide at around 350 °C (Zheng et al., 2014). The decomposition reaction as below:

$$Mg(OH)_2 \xrightarrow{\Delta} MgO + H_2O\uparrow \quad (2)$$

Based on the ash amounts obtained from kenaf fibers and MH-NFs, the MH contents were calculated as follows:

$$C_{\mathrm{Mg(OH)_2}} = \frac{(Ash_{\mathrm{Mg(OH)_2/fiber}} - Ash_{\mathrm{fiber}})}{(M_{\mathrm{MgO}}/M_{\mathrm{Mg(OH)_2}} - Ash_{\mathrm{fiber}})} \times 100\% \quad (3)$$

where $C_{\mathrm{Mg(OH)2}}$ is the MH content of MH-NF; $Ash_{\mathrm{Mg(OH)2/fiber}}$ is the ash content of MH-NF; $Ash_{\mathrm{fiber}}$ is the ash content of control kenaf fiber (3.7%); $M_{\mathrm{Mg(OH)2}}$ and $M_{\mathrm{MgO}}$ are the molecular weights (58.3 and 40.3 g mol$^{-1}$, respectively). It was assumed that no chemical interaction occurred between NFs (including their derivatives) and MH (including their derivatives) during the thermal decomposition.

### 2.3. *Vacuum bag resin transfer molding process*

Five natural fiber-reinforced composites (NFRCs) and five MH impregnated NFRCs (MH-NFRCs) with a size of approximate 100 (width) × 165 (length) × 3 (thickness) mm were manufactured. The NFRCs and MH-NFRCs were fabricated with the untreated NF and MH-NFs though the VBRTM process, using the UPS resin (1.5% t-BP) (Xia et al., 2015a). The flexible polyethylene vacuum bag and peer ply were used to wrap the kenaf preform. The wrapped assembly was placed on the rigid metal mold and the air in the assembly was expelled using the vacuum pump. After the system was vacuumed and all air leaks were eliminated, the resin was flowed through the preform. A vacuum pressure of 1.3 – 1.6 kPa was provided for driving the resin to impregnate the reinforcement preform. A lab-size hot press with approximate 13 MPa pressure was used to compress and cure the composites. The resin-impregnated preform was cured at 100 °C and then 150 °C for 2 h, respectively. The vacuum bag and peer ply were detached from the assembly after the system was cooled down. The prepared composite specimens were placed in a conditioning room (humidity: 50 ± 2%; temperature: 20 ± 3 °C) for approximate 30 d to reach an equilibrium constant weight before the mechanical property measurements.

### 2.4. *Mechanical tests*

Tensile tests were performed in according with the ASTM D638 standard. The AGS-X universal testing machine (maximum capacity: 10 kN) from Shimadzu Corp., Japan, was employed for the tests. A pair of grips with non-shift wedge (maximum capacity: 5kN) was used for clamping the specimens. The axial extensometer (Model 3542) from Epsilon Technology Corp., USA, was used for determining the strain changes during the tests. Using a table band saw, twelve specimens of each composite were sized to have dog-bone like structures, with entire dimensions of 19 (width) × 165 (length) × ~3 (thickness) mm and the narrow-section dimensions of 57 (length) × 13 (width) × ~3 (thickness) mm. The crosshead speed of the tensile tests was preset to be 1.3 mm min$^{-1}$. The tensile properties, including tensile strength, modulus, and elongation at break, were determined from the stain-stress curves from the tests.

Three-point bending tests (or flexural tests) were also carried out by the AGS-X universal testing machine with a 3-point bending kit (maximum capacity: 10 kN). Twelve specimens sized 25 (width) × 160 (length) × ~3 (thickness) mm were cut from each composite for the tests. In accordance with the ASTM D1037 standard, a span of 50 mm and a crosshead speed of 5 mm min$^{-1}$ were used in the tests. From the strain-stress curves, the modulus of elasticity and rupture, and flexural strain at break were determined in terms of Eqs. (4) – (6), respectively.

$$\text{Modulus of elasticity} = \frac{\mathrm{L^3m}}{\mathrm{4bd^3}} \quad (4)$$

$$\text{Modulus of rupture} = \max\left(\frac{3PL}{2bd^2}\right) \quad (5)$$

$$\text{Flexural strain at break} = \max\left(\frac{6Dd}{L^2}\right) \quad (6)$$

where L = length of support span; m = slope of the tangent to the initial straight-line portion of the load-deflection curve; b = width of beam tested; d = depth; P = load at a given point on the load-deflection curve; D = maximum deflection of the center of the beam.

*2.5. Microtopography analysis*

The samples, including the NFRC and MH13.3%-NFRC, were cut from the fracture failure sections of the tensile specimens and then sputtering-coated with gold for 1 min before the environmental scanning electron microscope (SEM) observation. The fracture failure surfaces of the tensile samples were examined using the Quanta 200 SEM. The accelerating voltage was set to be 20 kV, and the magnifications were 250× and 500× for the selected SEM images.

*2.6. Water absorptions*

The samples were placed in the chamber for approximate 30 days utile reaching an equilibrium constant, before the tests of moisture contents, thickness swellings (TSs), and water absorptions (WAs). According to the ASTM D4442 standard, the equilibrium moisture contents of the NFRCs and MH-NFRCs were determined using a conditioning room (see Section 2.3). The samples with a dimension of 25 (width) × 25 (length) × ~3 (thickness) mm were cut and five replicates were conducted. The submersion tests of TS and WA were performed in terms of the standard method described in the ASTM D1037. TSs and WAs of each sample were measured after the submersion of 2, 4, 8, 16, 24, 48, 72, and 120 h, respectively.

**3. Results and Discussion**

*3.1. Composites fabricated from in-situ magnesium hydroxide impregnated kenaf fibers*

The MH-NFs with four different MH contents of impregnation were prepared. Table 1 shows the compositions of untreated NF and MH-NFs. Using different amounts of $MgCl_2$ solutions (0.05, 0.1, 0.2, and 0.4 mol $g^{-1}$, respectively) during the *in-situ* impregnation, various amounts of MH were loaded on to the NF. In terms of Eq. (3), the MH loading amounts were calculated to be 7.1%, 10.3%, 13.3%, and 16.8%, respectively, and the corresponding fibers were named MH7.1%-NF, MH10.3%-NF, MH13.3%-NF, and MH16.8%-NF, respectively (Table 1).

**Table 1.** Compositions of magnesium hydroxide impregnated kenaf fibers.

| | Kenaf fiber (%) | Magnesium hydroxide (%) [c] |
|---|---|---|
| NF [a] | 100 | 0 |
| MH7.1%-NF [b] | 92.9 | 7.1 |
| MH10.3%-NF | 89.7 | 10.3 |
| MH13.3%-NF | 86.7 | 13.3 |
| MH16.8%-NF | 83.2 | 16.8 |

***Notes:*** [a] NF = natural fiber; [b] MH = magnesium hydroxide; [c] Magnesium hydroxide contents were calculated in terms of Eq. (3).

The NFRCs were fabricated by means of VBRTM process from five different types of fibers, including NF, MH7.1%-NF, MH10.3%-NF, MH13.3%-NF, and MH16.8%-NF. The densities and compositions of corresponding composites (namely, NFRC, MH7.1%-NFRC, MH10.3%-NFRC, MH13.3%-NFRC, and MH16.8%-NFRC) are shown in Table 2. The UPR content of NFRC was 33.3%, which was increased to be 35.4 – 35.7% after using MH-NF. The kenaf fiber and MH amounts of the composites are shown in Table 2. Compared to the NFRC (1159.4 kg $m^{-3}$), the densities of MH-NFRC were increased to be 1307.6 – 1365.9 kg $m^{-3}$ with an increase of 12.8 – 17.8%. It was mainly because of the addition of inorganic particles in the composites, which owned much higher density (2.34 g $cm^{-3}$) than that of both kenaf fibers (1.44 g $cm^{-3}$) and UPR (1.12 g $cm^{-3}$) (Xia et al., 2016c). It was revealed that the density increased with the increase in MH content (Table 2). Furtherly, the imagination of inorganic particles could reduce the porosity, which also increased the density of composites (Xia et al., 2016a).

**Table 2.** Densities and compositions of fiber-reinforced composites.

| Specimen | Density | Components (%) | | |
|---|---|---|---|---|
| | (kg $m^{-3}$) | UPR [d] | Kenaf fiber | Magnesium hydroxide |
| NFRC [a] | 1159.4 (44.5) [c] | 33.3 (5.2) | 66.7 (5.2) | - |
| MH7.1%-NFRC [b] | 1307.6 (20.5) | 35.6 (5.7) | 59.8 (5.3) | 4.6 (0.4) |
| MH10.3%-NFRC | 1319.8 (12.3) | 35.7 (3.1) | 57.7 (2.8) | 6.7 (0.3) |
| MH13.3%-NFRC | 1330.3 (13.6) | 35.6 (3.5) | 56.1 (3.1) | 8.3 (0.5) |
| MH16.8%-NFRC | 1365.9 (25.7) | 35.4 (4.2) | 53.8 (3.5) | 10.8 (0.7) |

***Notes:*** [a] NFRC = natural fiber-reinforced composite; [b] MH = magnesium hydroxide; [c] mean (standard deviation); [d] UPR = unsaturated polyester resin.

### *3.2. Tensile and flexural properties*

To examine mechanical properties of composites, three-point bending and tensile tests were performed and the results are listed in Table 3. Compared to that of NFRC, the bending properties of MH-NFRC, namely, modulus of elasticity and rupture, and flexural strain at break, were increased by 20.1–42.6%, 55.0–73.9%, and 39.4–57.3%, respectively. The tensile properties, namely, tensile modulus, strength and elongation at break, showed the increases of 0–20.2%, 24.0–54.6%, and 170.7–248.8%, respectively. The ultimate strengths (including modulus of rupture and tensile strength) of MH-NFRC containing 6.7–10.8% MH showed no significant changes (ANOVA test, *P-values* = 0.90 and 0.57, respectively), but higher than those of NFRC and MH7.1%-NFRC. It was indicated that the loading amount did not significantly affect the ultimate strengths of the composites made from the fibers with 6.7% MH. In Table 3, MH13.3%-NFRC owned the highest modulus of rupture (118.8 MPa) and tensile strength (68.9 MPa), which were significantly increased by 73.9% and 54.6% at $\alpha = 0.001$ level (ANOVA test, *P-values* = $2.53 \times 10^{-10}$ and $3.87 \times 10^{-8}$), respectively, compared with those of NFRC (68.3 MPa and 44.5 MPa). Compared to the aluminum hydroxide impregnated composites (106.3 MPa

and 60.6 MPa) (Xia et al., 2016d), the modulus of rupture and tensile strength of MH13.3%-NFRC were showed better values, indicating that the impregnation of MH endowed better strengths to the NFRC than aluminum hydroxide.

**Table 3.** Results from three-point bending and tensile tests of fiber reinforced composites.

| Specimen | Three-point bending tests | | | Tensile tests | | |
|---|---|---|---|---|---|---|
| | Modulus of elasticity (GPa) | Modulus of rupture (MPa) | Flexural strain at break (%) | Tensile modulus (GPa) | Tensile strength (MPa) | Tensile elongation at break (%) |
| NFRC [a] | 6.9 (0.6) [c] | 68.3 (6.3) | 1.1 (0.3) | 10.7 (1.0) | 44.5 (3.7) | 1.1 (0.5) |
| MH7.1%-NFRC [b] | 8.3 (0.5) | 105.9 (16.0) | 1.6 (0.2) | 10.2 (0.3) | 55.2 (3.2) | 3.1 (0.3) |
| MH10.3%-NFRC | 8.4 (0.2) | 111.2 (13.7) | 1.7 (0.1) | 11.0 (0.3) | 63.9 (3.6) | 3.2 (0.3) |
| MH13.3%-NFRC | 9.4 (0.2) | 118.8 (11.3) | 1.5 (0.1) | 10.7 (0.4) | 68.9 (2.5) | 4.0 (0.2) |
| MH16.8%-NFRC | 9.9 (0.3) | 115.3 (28.2) | 1.7 (0.5) | 12.8 (0.1) | 64.4 (7.3) | 3.2 (0.7) |

***Notes:*** [a] NFRC = natural fiber-reinforced composite; [b] MH = magnesium hydroxide; [c] mean (standard deviation).

### *3.3. Fracture surfaces investigation*

Fig. 1 shows the micromorphology of tensile fracture surfaces of NFRC and MH13.3%-NFRC. It was observed that NFRC images had many long pullout fibers and bundles (Fig. 1a). However, relatively shorter pullout fibers and more simultaneous failures occurred for the MH13.3%-NFRC (Fig. 1b). This finding was similar with the previous studies ($CaCO_3$-impregnated NFRC using polypropylene (PP) as matrix (Shi et al., 2011) and $CaCO_3$-impregnated NFRCs with UPR as resin (Xia et al., 2015b). As shown in Fig. 1b, the MH13.3%-NFRC images do not illustrate any fiber bundle, indicating the awfully improvement of interfacial compatibility between the reinforcing fillers (kenaf fibers) and UPR matrix. Furthermore, the pullout fibers of NFRC were much longer than that of MH13.3%-NFRC, specifying the poor adhesion between the pullout fibers and resin matrix, and then resulting in the inferior tensile strength of NFRC (Xia et al., 2016a).

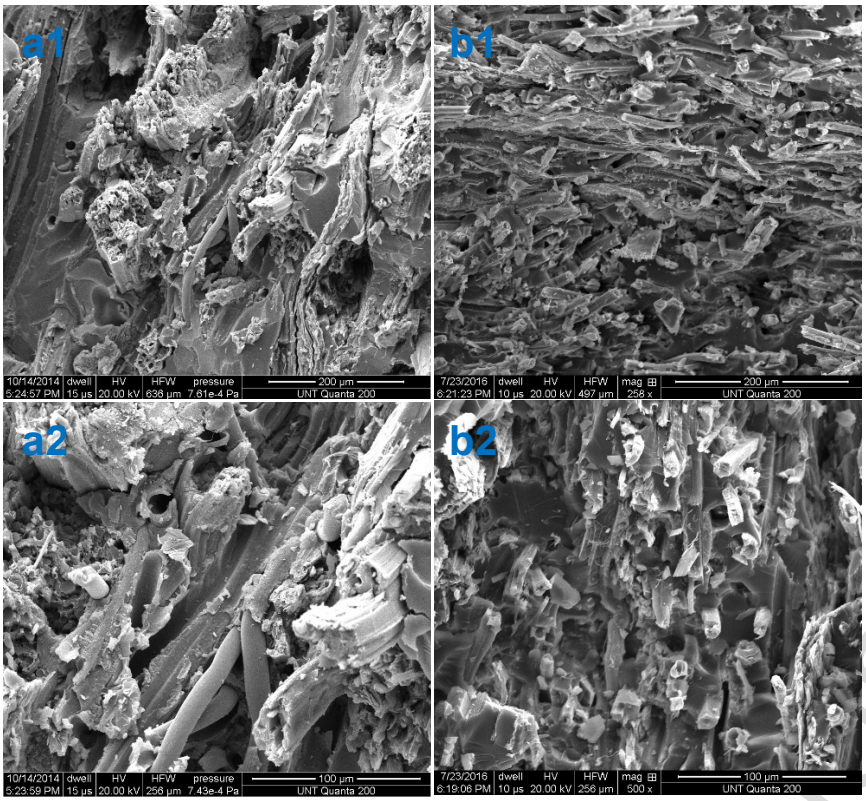


**Fig. 1.** SEM images of the tensile fracture surfaces of the composites made from regular natural fibers (NFRC) (a) and magnesium hydroxide impregnated natural fibers (MH13.3%-NFRC) (b).

*3.4. Water-resistant properties*

The TS results of the NFRC and MH-NFRCs are presented in Fig. 2 for a comparison. Obviously, the TSs of the composites (MH-NFRCs) were dramatically reduced after the impregnation of MH, compared with the control NFRC (Fig. 2a). The 24-h TSs of NFRC, MH7.1%-NFRC, MH10.3%-NFRC, MH13.3%-NFRC, and MH16.8%-NFRC were 19.7%, 2.8%, 3.4%, 3.1%, and 3.8%, respectively (Fig. 2b). Compared to the NFRC, the 24-h TS of MH13.3%-NFRC that owned the highest mechanical properties was significantly reduced by 84.2% (Anova test, $\alpha = 0.001$, *P-value* = $1.76 \times 10^{-4}$).

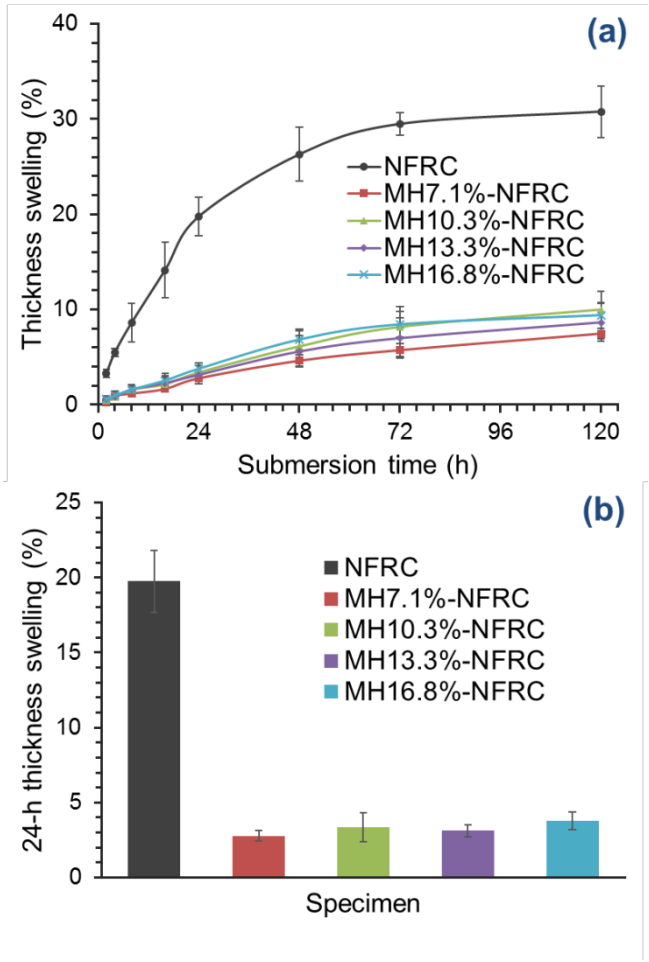


**Fig. 2.** Thickness swelling curves (a) and 24-h thickness swellings (b) of the fabricated composites.

The moisture contents of NFRC, MH7.1%-NFRC, MH10.3%-NFRC, MH13.3%-NFRC, and MH16.8%-NFRC were 5.8 ± 0.2%, 1.6 ± 0.2%, 2.0 ± 0.2%, 1.7 ± 0.1%, and 2.3 ± 0.2%, respectively, after the conditioning. It was showed that the moisture contents of MH-NFRCs were reduced by 59.8 – 72.0%, compared with that of NFRC. The curves of WAs of NFRC and MH-NFRCs are presented in Fig. 3a. Like the results of TS, the reductions of WAs of MH-NFRCs were dramatic, compared with that of NFRC. The 24-h WAs of the fabricated composites are compared in Fig. 3b, which were 18.3% (NFRC), 2.7% (MH7.1%-NFRC), 3.4% (MH10.3%-NFRC), 2.9% (MH13.3%-NFRC), and 2.9% (MH16.8%-NFRC), respectively. Compared to NFRC, the 24-h WA of MH13.3%-NFRC that had the optimal mechanical properties was significantly reduced by 83.9% analyzed by Anova test at $\alpha = 0.001$ level (*P-value* = $2.90 \times 10^{-4}$).

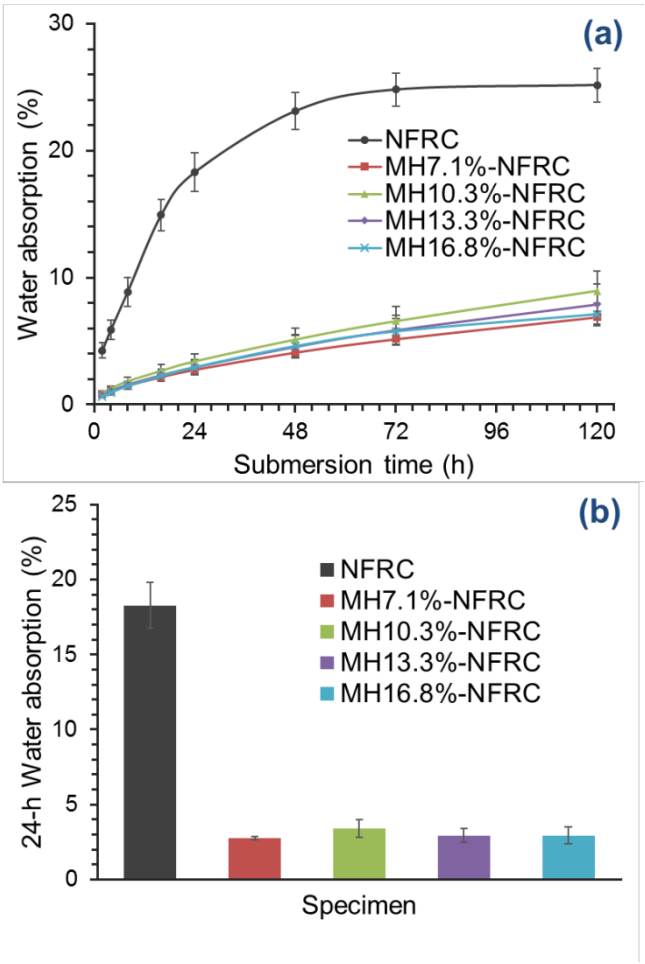


**Fig. 3.** Water absorption curves (a) and 24-h water absorptions (b) of fiber-reinforced composites.

Figs. 2 and 3 show that, after the impregnation of MH inorganic particles onto kenaf fibers, the water resistances of the composites were dramatically improved through the tests of TSs and WAs. Obviously, the major reason could be contributed by the MH inorganic particle impregnation. Benefited from the hydrogen bonding between the MH and kenaf fibers, the MH particles stick onto the surfaces of kenaf fibers so that clogged plenty of hydrophilic groups (hydroxyl) in kenaf fibers. The depositing of MH particles on the fiber surfaces could hugely cut down the contacts between the water molecules and kenaf fibers, presenting as improved water-resistant property. This phenomenon was also investigated when the inorganic particles of calcium carbonate and aluminum hydroxide were employed for improving the water resistances of NF composites (Xia et al., 2016d). Though MH is hydrophilic and its water contact angle is almost 0° (Hu and Deng, 2006), the MH owns an extremely low solubility (insolubility) of 0.00064 g in 100 mL water at 25 °C (Wikipedia) and non-swelling in water. These behaviors, including insolubility and non-swelling, of the MH particles in the water indicated that the MH particles would not absorb much moisture. Thereby, the coating of MH on the fiber surfaces would only prevent the water contacting with fibers but not absorb water itself.

### *3.5. MH13.3%-NFRC vs. GF-SMC*

#### 3.5.1. Comparisons of physical parameters, moisture contents and water resistance

Although GF-SMC is widely employed as automotive panels currently, the environmental concern has been arisen because of its inherent composition. Compared to the GFs, the kenaf fibers are lighter,

more sustainable, economical, and eco-friendly, which has been attracted an increasing attention (Akil et al., 2011). The properties of MH13.3%-NFRC and SLI 323IF GF-SMC (Meridian Automotive Systems Inc., USA) with a 2.5 mm thickness were compared. Meridian's SLI 323 GF-SMCs were used as outer door panels, roof bow and tonneau of the Chevrolet Corvette, and the front roof panel, tonneau and fuel filler door of the Cadillac XLR (Composites World Magazine Staff, 2006). The physical parameters, moisture contents and 24-h WAs of the GF-SMC and MH13.3%-NFRC are compared in Table 4. The MH13.3%-NFRC owned the optimal mechanical properties in all NFRCs with different contents of MH (Table 3) and 26.2 % lower density than GF-SMC, benefiting to decrease the automobile weight. Due to the numerous hollow spots in NFs which might capture more resin, the resin content of the MH13.3%-NFRC was higher than GF-SMC (37.6% *vs.* 26%). And the MH13.3%-NFRC owned much higher fiber content than GF-SMC (65.2% *vs.* 28%). It was mainly considered that the MH13.3%-NFRC owned less filling minerals than GF-SMC (8.3% vs. 46%) (Table 4).

**Table 4.** Comparisons of the physical parameters, moisture contents and 24-h water resistance of GF-SMC and MH13.3%-NFRC.

| Specimen | Density ($kg\ m^{-3}$) | Components (wt.%) | | | Moisture content (%) | 24-h WA [g] (%) |
|---|---|---|---|---|---|---|
| | | UPR [d] | Fiber [e] | Mineral [f] | | |
| GF-SMC [a] | 1801.8 (27.1) [c] | 26 | 28 | 46 | 0.3 (0.0) | 1.1 (0.3) |
| MH13.3%-NFRC [b] | 1330.3 (13.6) | 37.6 (3.5) | 54.1 (3.1) | 8.3 (0.5) | 1.7 (0.1) | 2.9 (0.5) |

***Notes:*** [a] GF-SMC = glass-fiber sheet molding compound; [b] MH = magnesium hydroxide, NFRC = natural fiber-reinforced composite; [c] mean (standard deviation); [d] UPR = unsaturated polyester resin; [e] glass fiber for the GF-SMC, kenaf fiber for the MH13.3%-NFRC; [f] minerals (mainly in calcium carbonate) for GF-SMC, magnesium hydroxide for MH13.3%-NFRC; WA = water absorption.

### 3.5.2. Comparison of the mechanical properties

A comparison of the mechanical properties and specific ultimate strengths between GF-SMC and MH13.3%-NFRC are illustrated in Fig. 4. The modulus of elasticity and rupture, flexural strain at break, and tensile modulus, strength and elongation at break of GF-SMC were measured to be 10.2 GPa, 138.2 MPa, 2.5%, 13.7 GPa, 85.6 MPa, and 3.7%, respectively. After using MH impregnated kenaf fibers, these mechanical properties of MH13.3%-NFRC were 91.9%, 85.9%, 62.2%, 78.2%, 80.5%, and 115.8% of the values of GF-SMC, respectively (Fig. 4). To compare the MH13.3%-NFRC and GF-SMC using their normalized densities, the specific ultimate strengths, including specific modulus of rupture and tensile strength, were calculated according to Eq. (7).

$$Specific\ ultimate\ strength = \frac{Ultimate\ strength}{Specific\ gravity} \quad (7)$$

The specific gravities of MH13.3%-NFRC and GF-SMC were 1.33 and 1.80 (Table 4), respectively. The specific modulus of ruptures of MH13.3%-NFRC and GF-SMC were calculated to be 89.3 MPa and 76.7 MPa, respectively, and their specific tensile strengths were 51.8 MPa and 47.5 MPa, respectively. The comparisons of specific ultimate strengths between MH13.3%-NFRC and GF-SMC are illustrated in Fig. 4 (highlighted in green dash line). It was shown that the specific modulus

of rupture and tensile strength of MH13.3%-NFRC were 116.4% and 109.0% of the values of GF-SMC. Considering the comparison results between MH13.3%-NFRC and GF-SMC, the MH13.3%-NFRC was comparable with the commercial GF-SMC used as automotive panels.

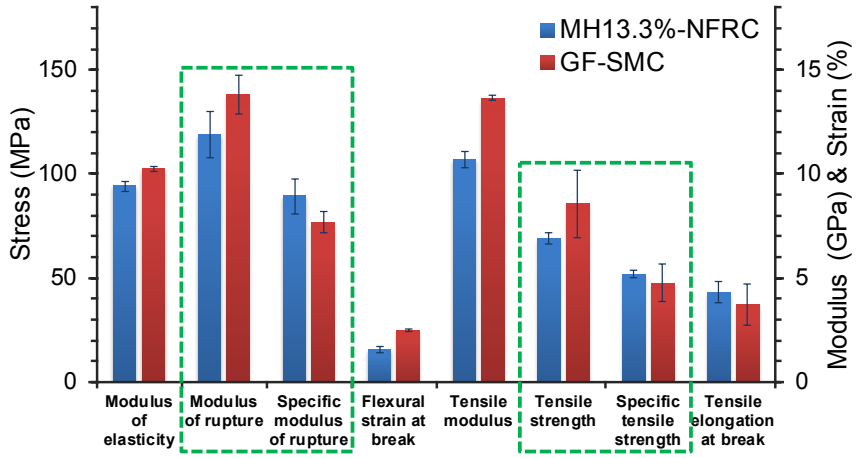


**Fig. 4.** Mechanical properties and specific ultimate strengths of MH13.3%-NFRC and GF-SMC.

### 3.5.3. Comparison of the energy consumption

The energy consumption of production of 1 kg of kenaf fibers is 15 MJ, while 1 kg of GFs need 54 MJ (Akil et al., 2011). Even incorporating the energy cost during the treatment of kenaf fibers, which is roughly estimated to be 15% of energy consumption, the total energy consumption of kenaf fibers was calculated to be 17.25 MJ. Compared to GFs, the energy consumption of kenaf fibers production was decreased by 68.0%, presenting a great reduction. Apart from the fibers, another main energy consumption of the composites is from the resin used. The production of 1 kg of polyester resin will consume approximate 46 MJ energy (Fletcher, 2013). Compared to the fibers and resins, the energy consumption of mineral is much less, for instance, the consumed energy for producing 1 kg of lime is approximate 6.25 MJ (Stubbles, 2000). It was assumed to be the energy consumption of the minerals in the composites.

Based on the density and components of the composites (Table 4), the absolute weights of fibers, resins, and minerals in 1 $m^3$ of the MH13.3%-NFRC/GF-SMC composites were 719.7/504.5, 500.2/468.5, and 110.4/828.8 kg, respectively. By incorporating with the corresponding energy consumptions, the total energy consumptions of the composites and individual values of each component are presented in Fig. 5. It need to be noticed that the energy cost of composite fabrication was not included. The total energy consumption of MH13.3%-NFRC was 36.1 GJ $m^{-3}$ composite, which was 33.1% lower than that of GF-SMC (54.0 GJ $m^{-3}$ composite). The main reason could be the dramatical reduction of energy used in kenaf fibers manufacturing compared with GFs.

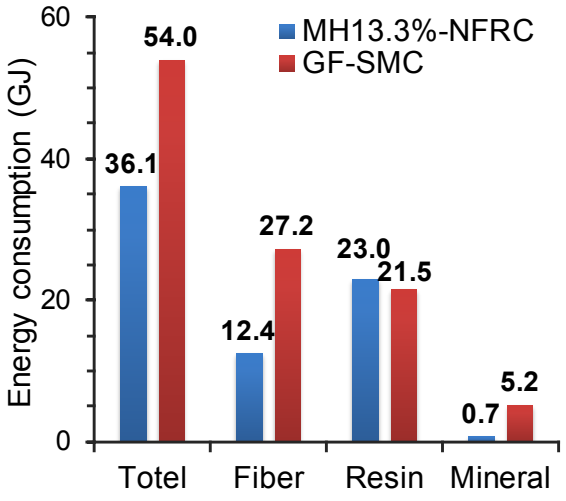


Fig. 5. Comparison of energy consumption of 1 $m^3$ MH13.3%-NFRC and GF-SMC.

### 3.5.4. Comparison of the life-cycle assessment

The comparison of LCA between NFRC and GF-SMC was conducted using the SimaPro software. The functional unit had been defined as one cubic meter for both composites. The eco-indicator 99 points were calculated by normalization and weighting of the damage factors. The eco-indicator single score is helpful in the search for more environmentally friendly design alternatives. One point on the eco-indicator scale represents one thousandth of the annual environmental load from one average European person (Goedkoop and Spriensma, 2001). Using method of eco-indicator 99 points (Pt) in the Simapro 8.2 software, the Environmental burdens of GF-SMC and NFRC were calculated to be 0.0032 Pt and 0.00247 Pt, respectively, which demonstrated that a reduction of 22.8% was achieved as kenaf replaced fiberglass. The total environmental impacts between GF-SMC and MH13.3%-NFRC were compared using Simapro and the results of impact categories are presented in Table 5.

**Table 5.** LCA comparisons of total environmental impacts between GF-SMC and MH13.3%-NFRC.

| Environmental impact category | GF-SMC | NFRC[a] | Reduction (%) |
|---|---|---|---|
| Global warming (g. $CO_2$ eq.) | $1.95 \times 10^3$ | $1.54 \times 10^3$ | 20.92 [b] |
| Acidification ($H^+$ moles eq.) | $4.29 \times 10^{-1}$ | $3.62 \times 10^{-1}$ | 15.56 |
| Human Health (HH) cancer (g. $C_6H_6$ eq.) | 6.39 | 4.86 | 23.84 |
| HH noncancer (g. $C_7H_7$ eq.) | $1.22 \times 10^5$ | $8.47 \times 10^4$ | 30.90 |
| HH criteria air pollutants (Micro DALYs) | $2.83 \times 10^{-1}$ | $1.84 \times 10^{-1}$ | 34.96 |
| Eutrophication (g. N. eq.) | 5.39 | 4.53 | 16.03 |
| Ecotoxicity (g. 2,4-D eq.) | $1.13 \times 10^1$ | 7.35 | 34.76 |
| Smog (g. NOx eq.) | 5.00 | 3.50 | 29.91 |
| Natural resource depletion (MJ surplus) | 4.42 | 3.82 | 13.66 |
| Habitat alteration (T&E count) | $1.89 \times 10^{-14}$ | $1.42 \times 10^{-14}$ | 24.68 |
| Water intake (Liters) | $5.86 \times 10^1$ | $2.82 \times 10^1$ | 51.91 |
| Ozone depletion (g. CFC-11 eq.) | $7.01 \times 10^{-4}$ | $1.89 \times 10^{-4}$ | 72.99 |

***Notes:*** [a] Natural fiber-reinforced composite with 13.3% magnesium hydroxide was used here; [b] The reduction was calculated by comparing the environmental impact of NFRC and GF-SMC.

## 4. Conclusions

The results of this study indicated that the newly developed kenaf fiber composites is potential to replace GF-SMC used as automotive panels. The mechanical properties of NFRCs were dramatically enhanced using the MH-NFs and VBRTM technology. Among the five types of tested composites, MH13.3%-NFRC owned the highest modulus of rupture (118.8 MPa) and tensile strength (68.9 MPa), which were counted increases of 73.9% and 54.6%, respectively, compared with those of regular NFRC (68.3 MPa and 44.5 MPa). The SEM observation revealed greatly improved interfacial compatibility between kenaf fibers and polyester resin after impregnating MH into the kenaf fibers, resulting in the significantly improvement in mechanical performance of NFRC. Compared to the regular NFRC, the 24-h TS and WA of new developed MH13.3%-NFRC were significantly reduced by 84.2% and 83.9%, respectively. Compared to GF-SMC, the tensile and bending properties of MH13.3%-NFRC were comparable. When the composite density was factored in the comparison between MH13.3%-NFRC and GF-SMC, the specific modulus of rupture and tensile strength of MH13.3%-NFRC were 116.4% and 109.0% of the values of GF-SMC. Apart from the mechanical properties, the MH13.3%-NFRC exhibited reduced energy consumption and environmental impacts, compared with GF-SMC. The calculation of energy consumption revealed that 33.1% of energy would be saved in the NFRC fabricating process compared with GF-SMC manufacturing. The LCA results indicated that the environmental burdens of the composites were reduced by 22.8%. All major indices of environmental impacts were reduced when kenaf fibers were used to replace GFs. Compared to the traditional GF-SMC, the total Global warming, Acidification, HH cancer, HH noncancer, HH criteria air pollutants, Eutrophication, Ecotoxicity, Smog, Natural resource depletion, Habitat alteration, Water intake and Ozone depletion of the NFRCs reduced by 20.92, 15.56, 23.84, 30.90, 34.96, 16.03, 34.76, 29.91, 13.66, 24.68 and 51.91 %, respectively. The comparable mechanical properties, and reduced energy consumption and environmental impacts endowed the great potential to the NFRC for replacing GF-SMC in automobile applications.

## Acknowledgement

This research was supported by National Science Foundation (NSF) CMMI 1247008.

**References**

Akil, H.M., Omar, M.F., Mazuki, A.A.M., Safiee, S., Ishak, Z.A.M., Abu Bakar, A., 2011. Kenaf fiber reinforced composites: A review. Mater. Design. 8-9, 4107-4121

AL-Oqla, F.M., Sapuan, S.M., 2014. Natural fiber reinforced polymer composites in industrial applications: feasibility of date palm fibers for sustainable automotive industry. J. Clean. Prod., 347-354

Alves, C., Ferrao, P.M.C., Silva, A.J., Reis, L.G., Freitas, M., Rodrigues, L.B., Alves, D.E., 2010. Ecodesign of automotive components making use of natural jute fiber composites. J. Clean. Prod. 4, 313-327

Ardente, F., Beccali, M., Cellura, M., Mistretta, M., 2008. Building energy performance: A LCA case study of kenaf-fibres insulation board. Energy Build. 1, 1-10

Ashori, A., 2008. Wood-plastic composites as promising green-composites for automotive industries!. Bioresour. Technol. 11, 4661-4667

Bledzki, A.K., Letman, M., Viksne, A., Rence, L., 2005. A comparison of compounding processes and wood type for wood fibre - PP composites. Composites Part A. 6, 789-797

Boonterm, M., Sunyadeth, S., Dedpakdee, S., Athichalinthorn, P., Patcharaphun, S., Mungkung, R., Techapiesancharoenkij, R., 2016. Characterization and comparison of cellulose fiber extraction from rice straw by chemical treatment and thermal steam explosion. J. Clean. Prod., 592-599

Chandrasekar, M., Ishak, M.R., Sapuan, S.M., Leman, Z., Jawaid, M., 2017. A review on the characterisation of natural fibres and their composites after alkali treatment and water absorption. Plast. Rubber Compos. 3, 119-136

Chen, Q., Ting Linghu, Gao, Y., Wang, Z., Liu, Y., Du, R., Zhao, G., 2017. Mechanical properties in glass fiber PVC-foam sandwich structures from different chopped fiber interfacial reinforcement through vacuum-assisted resin transfer molding (VARTM) processing. Composites Sci. Technol., 202-207

Claramunt, J., Fernandez-Carrasco, L.J., Ventura, H., Ardanuy, M., 2016. Natural fiber nonwoven reinforced cement composites as sustainable materials for building envelopes. Constr. Build. Mater., 230-239

Composites World Magazine Staff, 2006. 2006 Corvette Incorpora tes Reformula ted " pop-free" SMC, http://www.corvetteactioncenter.com/tech/knowledgebase/article/2006-corvette-technical-article-2006-corvette-incorporates-reformulated-pop-free-smc-360.html (Accessed on 2/9/2018)

Dahlke, B., Larbig, H., Scherzer, H.D., Poltrock, R., 1998. Natural fiber reinforced foams based on renewable resources for automotive interior applications. J. Cell. Plast. 4, 361-379

Fletcher, K., 2013. Sustainable fashion and textiles: design journeys. Routledge

Goedkoop, M., Spriensma, R., 2001. The eco-indicator 99: A damage oriented method for life cycle impact assessment. Methodology Report., 3rd ed. PRé Consultants b.v., Amersfoort, The Netherlands

Holbery, J., Houston, D., 2006. Natural-fiber-reinforced polymer composites applications in automotive. JOM. 11, 80-86

Hu, H., Deng, X., 2006. Preparation and properties of superfine Mg(OH)2 flame retardant. T. Nonferr. Metal. Soc. 2, 488-492

Koh, P., Yan, J., Teja, A., 2011. Precipitation and growth of magnesium hydroxide nanopetals on zeolite 4A surfaces. J. Cryst. Growth. 1, 56-63

Korol, J., Burchart-Korol, D., Pichlak, M., 2016. Expansion of environmental impact assessment for eco-efficiency evaluation of biocomposites for industrial application. J. Clean. Prod., 144-152

Koronis, G., Silva, A., Fontul, M., 2013. Green composites: A review of adequate materials for automotive applications. Composites Part B. 1, 120-127

La Rosa, A.D., Recca, G., Summerscales, J., Latteri, A., Cozzo, G., Cicala, G., 2014. Bio-based versus traditional polymer composites. A life cycle assessment perspective. J. Clean. Prod., 135-144

Marsh, G., 2003. Next step for automotive materials. Mater. Today. 4, 36-43

Mendonca Sales, R.d.C., Gusmao, S.R., Gouvea, R.F., Chu, T., Fernandez Marlet, J.M., Candido, G.M., Donadon, M.V., 2017. The temperature effects on the fracture toughness of carbon fiber/RTM-6 laminates processed by VARTM. J. Composite Mater. 12, 1729-1741

Pervaiz, M., Sain, M., 2003. Sheet-molded polyolefin natural fiber composites for automotive applications. Macromol. Mater. Eng. 7, 553-557

Pickering, K.L., Efendy, M.G.A., Le, T.M., 2016. A review of recent developments in natural fibre composites and their mechanical performance. Composites Part A, 98-112

Rebitzer, G., Ekvall, T., Frischknecht, R., Hunkeler, D., Norris, G., Rydberg, T., Schmidt, W., Suh, S., Weidema, B., Pennington, D., 2004. Life cycle assessment Part 1: Framework, goal and scope definition, inventory analysis, and applications. Environ. Int. 5, 701-720

Sadeghian, R., Gangireddy, S., Minaie, B., Hsiao, K., 2006. Manufacturing carbon nanofibers toughened polyester/glass fiber composites using vacuum assisted resin transfer molding for enhancing the mode-I delamination resistance. Composites Part A. 10, 1787-1795

Shi, J., Shi, S.Q., Barnes, H.M., Horstemeyer, M.F., Wang, G., 2011. Kenaf bast fibers-Part II: Inorganic nanoparticle impregnation for polymer composites. Int. J. Polym. Sci., 736474

Stubbles, J., 2000. Energy use in the US steel industry: a historical perspective and future opportunities. Energetics, Inc. Columbia, MD, https://www.energy.gov/sites/prod/files/2013/11/f4/steel_energy_use.pdf (Accessed on 2/9/2018)

Vaisanen, T., Das, O., Tomppo, L., 2017. A review on new bio-based constituents for natural fiber-polymer composites. J. Clean. Prod., 582-596

Wang, C., Cheng, H., Xian, Y., Wang, G., Zhang, S., 2017. Improving dynamic mechanical property of bamboo pulp fiber reinforced epoxy resin composite treated by nano calcium carbonate. Trans. Chin. Soc. Agr. Eng. 6, 281-287

Xia, C., Shi, S.Q., 2016. Self-activation for activated carbon from biomass: theory and parameters. Green Chem., 2063-2071

Xia, C., Shi, S.Q., Cai, L., Hua, J., 2015a. Property enhancement of kenaf fiber composites by means of vacuum-assisted resin transfer molding (VARTM). Holzforschung. 3, 307-312

Xia, C., Shi, S.Q., Cai, L., 2015b. Vacuum-assisted resin infusion (VARI) and hot pressing for CaCO3 nanoparticle treated kenaf fiber reinforced composites. Composites Part B, 138-143

Xia, C., Shi, S.Q., Wu, Y., Cai, L., 2016a. High pressure-assisted magnesium carbonate impregnated natural fiber-reinforced composites. Ind. Crop. Prod., 16-22

Xia, C., Yu, J., Shi, S.Q., Qiu, Y., Cai, L., Wu, H.F., Ren, H., Nie, X., Zhang, H., 2017. Natural fiber and aluminum sheet hybrid composites for high electromagnetic interference shielding performance. Composites Part B, 121-127

Xia, C., Zhang, S., Ren, H., Shi, S.Q., Zhang, H., Cai, L., Li, J., 2016b. Scalable fabrication of natural-fiber reinforced composites with electromagnetic interference shielding properties by incorporating powdered activated carbon. Materials. 1, 10

Xia, C., Garcia, A.C., Shi, S.Q., Qiu, Y., Warner, N., Wu, Y., Cai, L., Rizvi, H.R., D'Souza, N.A., Nie, X., 2016c. Hybrid boron nitride-natural fiber composites for enhanced thermal conductivity. Sci. Rep., 34726

Xia, C., Zhang, S., Shi, S.Q., Cai, L., Huang, J., 2016d. Property enhancement of kenaf fiber reinforced composites by in situ aluminum hydroxide impregnation. Ind. Crop. Prod., 131-136

Yan, L., Chouw, N., 2014. Natural FRP tube confined fibre reinforced concrete under pure axial compression: A comparison with glass/carbon FRP. Thin Wall. Struct., 159-169

Zamri, M.H., Osman, M.R., Akil, H.M., Shahidan, M.H.A., Ishak, Z.A.M., 2016. Development of green pultruded composites using kenaf fibre: influence of linear mass density on weathering performance. J. Clean. Prod., 320-330

Zheng, Y., Miao, J., Maeda, N., Frey, D., Linhardt, R.J., Simmons, T.J., 2014. Uniform nanoparticle coating of cellulose fibers during wet electrospinning. J. Mater. Chem. A. 36, 15029-15034

Zhu, Y., Wu, G., Zhang, Y., Zhao, Q., 2011. Growth and characterization of Mg(OH)(2) film on magnesium alloy AZ31. Appl. Surf. Sci. 14, 6129-6137

**Highlights**

- Composites were fabricated using $Mg(OH)_2$ impregnated kenaf fibers and polyester
- Dramatically enhanced mechanical properties using $Mg(OH)_2$-impregnated fibers
- Comparable properties with automotive glass-fiber sheet molding compound (GF-SMC)
- Energy consumption was decreased by 33.1% compared with GF-SMC
- Environmental impact was reduced by 22.8% from life-cycle assessment